Phase maps based on the Lorenz–Mie theory to optimize phase Doppler particle-sizing systems

Zilong Jiang

A phase Doppler particle-sizing system, whose main part is a two-beam laser interferometer, can be used to determine the size of scattering particles by measuring the phase differences between two signals detected by two detectors located in a scattered field. Important parameters of the receiving system to be selected include the off-axis angle, the elevation angle, and parameters of receiving apertures. A method is described for theoretically optimizing such measuring systems with the aid of so-called phase maps based on the Lorenz–Mie scattering theory. This method has been systematically studied and applied for cases of water droplets, metal particles, and droplets of weakly absorbing fluid. The results have shown that phase maps are direct, simple, and unique to interpret, and they provide an effective tool in setting up measuring systems. © 1997 Optical Society of America

Key words: Lorenz–Mie theory, light scattering, phase Doppler anemometry, particle sizing.

1. Introduction

Because of its reliability, nonintrusive property, and flexibility, phase Doppler anemometry (PDA) has been widely used to measure the size and velocity of particles in two-phase flows simultaneously.[1–4] In every application of the PDA technique, a set of proper measuring parameters must be selected to ensure reliable and correct measurements. In the phase Doppler method the particle size is related to the phase difference between two signals detected by two detectors located in the scattered field of a two-beam interferometer, and it is desired to have a simple linear relationship of the phase difference to the particle diameter. To this end one can determine the measuring parameters by applying the principles of geometrical optics so that the positions where reflection or refraction is dominant can be approximated.[2,5,6] However, this method is valid only if the particles are absorption free or strongly absorbing. The Lorenz–Mie theory,[7] in contrast, is valid for general cases in which the incident waves can be treated as plane waves and the scattering objects can be treated as spherical and homogeneous particles. This condition is normally satisfied in most PDA applications.

Much research has already been done to evaluate two-beam interferometric particle-sizing systems by using the Lorenz–Mie theory. The seminal research was that of Farmer,[8] who dealt with visibility in an on-axis scattering system of a small beam crossing angle. Chu and Robinson[9] also calculated scattered signals for on-axis detections. Hong and Jones[10] treated the case for small rectangular apertures at off-axis positions, and later Pendleton[11] implemented an integration scheme for circular apertures at arbitrary locations. These contributions formed the basis of calculating and evaluating a PDA system that has two receivers instead of one, and in which the phase difference between the two detected signals is included.[3,6,12,13] In addition, the intensity distribution at the aperture plane was examined and treated as a tool for understanding[5] and for parameter selection.[13]

In the PDA technique the phases instead of intensities are correlated with particle diameters, and the intensity distribution in the form of interference fringes moves as the particle moves through the measurement volume. Consequently, knowledge of the intensity distribution does not help considerably to select parameters as off-axis angles and elevation angles. The intensity is only a carrier of phase information and does not provide a simple and unique criterion for a suitable location of an aperture. The direct use of phase information in the design of PDA systems was utilized by Gréhan *et al.*[14] to judge ap-

The author is with the Changchun Institute of Optics and Fine Mechanics, State Key Laboratory of Applied Optics, 130022 Changchun, China.

Received 23 January 1995; revised manuscript received 6 February 1996.

0003-6935/97/061367-09$10.00/0

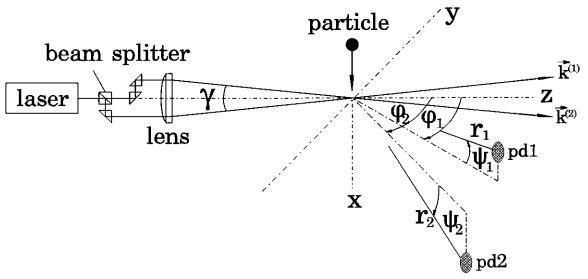

Fig. 1. PDA setup: γ, beam crossing angle; $\mathbf{k}^{(1)}$, $\mathbf{k}^{(2)}$, wave vectors of incident beams; r_1, r_2, detection distances; φ_1, φ_2, off-axis angles; ψ_1, ψ_2, elevation angles; pd1, pd2, photodetectors.

paratus sensitivity to particle trajectory effect and by Benzon and Buchhave to configurate measuring systems for the submicrometer size range.[15] The phase distribution in the receiving plane, which I have investigated[16] and which is presented here, provides, in contrast to that of intensity, an exclusive picture as to where the detectors should be positioned. Then the standard two-dimensional phase-size presentation[3,5,13] can be utilized to confirm the configuration and to calibrate the measuring system. Through the examples of water droplets, metal particles, and droplets from absorbing fluids, this method has been systematically examined. It has been determined that this method has the advantages of simplicity, directness, and uniqueness.

2. Basis of Phase Doppler Anemometry Setups

The main part of a phase Doppler anemometer is a two-beam scattering geometry, as shown in Fig. 1. An arbitrarily linearly polarized laser beam of angular frequency ω is split into two beams whose polarization directions can be changed if necessary. They intersect with a crossing angle γ at a region referred to as the interference volume or measurement volume. When a particle moves through this region it simultaneously scatters the two incident beams in all directions. Because the theoretical formulation of PDA can be found extensively in the literature, e.g., in Refs. 9, 12, and 17, only the results are summarized here. From the electromagnetic wave theory the observed intensity of the scattered field at position $\mathbf{r}$ is the magnitude of the time-averaged Poynting vector:

$$\mathbf{S}_s(\mathbf{r}, t) = [A + B \exp(-i\omega_D t) + B^* \exp(i\omega_D t)]\hat{\mathbf{r}}, \quad (1)$$

where

$$A = |\mathbf{E}_s{}^{(1)}(\mathbf{r})|^2 + |\mathbf{E}_s{}^{(2)}(\mathbf{r})|^2,$$
$$B = \mathbf{E}_s{}^{(1)}(\mathbf{r}) \cdot \mathbf{E}_s{}^{(2)*}(\mathbf{r}),$$
$$\omega_D = \Delta\omega^{(1)} - \Delta\omega^{(2)} = \mathbf{v} \cdot [\mathbf{k}^{(2)} - \mathbf{k}^{(1)}].$$

In these expressions the subscript s stands for the scattered field, superscript $(j) = (1, 2)$ denotes the related variables from the jth incident beam, $\mathbf{E}_s{}^{(1)}$ and $\mathbf{E}_s{}^{(2)}$ are the complex electric amplitudes of the scattered field and can be determined by applying the results of the Lorenz–Mie theory,[7,18] the asterisk denotes the conjugation of a complex variable, $\hat{\mathbf{r}}$ is the unit vector of $\mathbf{r}$, vectors $\mathbf{v}$, $\mathbf{k}^{(1)}$, and $\mathbf{k}^{(2)}$ are the velocity of the particle and wave vectors of the incident beams in the surrounding medium with $|\mathbf{k}^{(j)}| = 2\pi/\lambda = k$, respectively; ω_D is the Doppler frequency. Frequency shift $\Delta\omega^{(j)}$ is caused by the movement of the scattering particle, and

$$\omega^{(j)} = \omega + \Delta\omega^{(j)}. \quad (2)$$

Thus the intensity at position $\mathbf{r}$ is

$$I_s(\mathbf{r}, t) = A + 2(B_{\mathrm{Re}}{}^2 + B_{\mathrm{Im}}{}^2)^{1/2} \cos(\omega_D t + \Phi), \quad (3)$$

where

$$\Phi = -\tan^{-1}\left(\frac{B_{\mathrm{Im}}}{B_{\mathrm{Re}}}\right), \quad (4)$$

and B_{Re} and B_{Im} are the real and imaginary parts of function B. Phase function Φ and functions A and B depend only on position and the system arrangement, whereas intensity function I_s also depends on time t. For a different time t there is therefore a different distribution of intensity, or in other words the interference fringe pattern moves over the detector aperture if the velocity of the scattering particle $\mathbf{v} \neq 0$. Function Φ is considered as the basis of the method subsequently described.

If a detector with a receiving solid angle of $\Delta\Omega$ with respect to the scattering particle is placed in the scattered field, it receives a light power of

$$P_s(t) = \int_{\Delta\Omega} I_s(\mathbf{r}, t) r^2 \mathrm{d}\Omega, \quad (5)$$

where $r = |\mathbf{r}|$ is the distance between the scattering particle and the receiving element. By substituting Eq. (3) into Eq. (5), it follows that

$$P_s(t) = P_{\mathrm{dc}} + P_{\mathrm{ac}} \cos(\omega_D t + \bar{\Phi}),$$
$$= P_{\mathrm{dc}}[1 + V \cos(\omega_D t + \bar{\Phi})], \quad (6)$$

where

$$P_{\mathrm{dc}} = \int_{\Delta\Omega} A r^2 \mathrm{d}\Omega,$$
$$P_{\mathrm{ac}} = 2(\bar{B}_{\mathrm{Re}}{}^2 + \bar{B}_{\mathrm{Im}}{}^2)^{1/2},$$
$$\bar{\Phi} = -\tan^{-1}\left(\frac{\bar{B}_{\mathrm{Im}}}{\bar{B}_{\mathrm{Re}}}\right),$$
$$V = \frac{P_{\mathrm{ac}}}{P_{\mathrm{dc}}}. \quad (7)$$

In Eqs. (7) $\bar{B}_{\mathrm{Re}}$ and $\bar{B}_{\mathrm{Im}}$ are the real and imaginary parts of integration $\int_{\Delta\Omega} B r^2 \mathrm{d}\Omega$, P_{dc} and P_{ac} are the dc and ac parts of the detected power and V and $\bar{\Phi}$ are the visibility and phase of the signal received by one detector, respectively. Phase $\bar{\Phi}$ is a relative quantity, and if a second detector is located at a position

Table 1. Input Data

Parameter	Value
Wavelength in vacuum (μm)	0.488
Particle diameter (μm)	0.01 → 150
Refractive index of the medium	1.0
Half-beam crossing angle (deg)	0.955
Elevation angles (deg)	±2.4
Half-receiving angle of detectors (deg)	1.49

differing from that of the first one, the phase difference between the two signals can be uniquely determined and related to the size of the scattering particle. The quantities in Eqs. (7) are considered as the fundamentals of a PDA system.

3. Programs and Results

In finding suitable aperture positions of photodetectors, the geometrical optics is helpful for simple cases, e.g., for refracting or reflecting particles. If weak or mild absorption appears, the geometrical optics becomes invalid. Here an effective alternative method that uses phase maps and is based on the Lorenz–Mie theory is introduced.

The subroutine modified from MIEV0 written by Wiscombe[19] as the kernel to compute the scattered complex amplitudes has been integrated in the FORTRAN programs, which allows the use of only the downward recurrence. Two programs were developed. One is based on the formula of the nonintegrated phase function of Eq. (4) and was used to calculate phase distributions of the scattered light intensity on the aperture plane. The results are presented in the form of contours, called phase maps. The other program is based on the four variables in Eqs. (7), which are quantities integrated over the receiving aperture and the fundamentals in calculating a PDA instrument.

In PDA techniques the relationship between particle diameters and phase differences, the visibility,

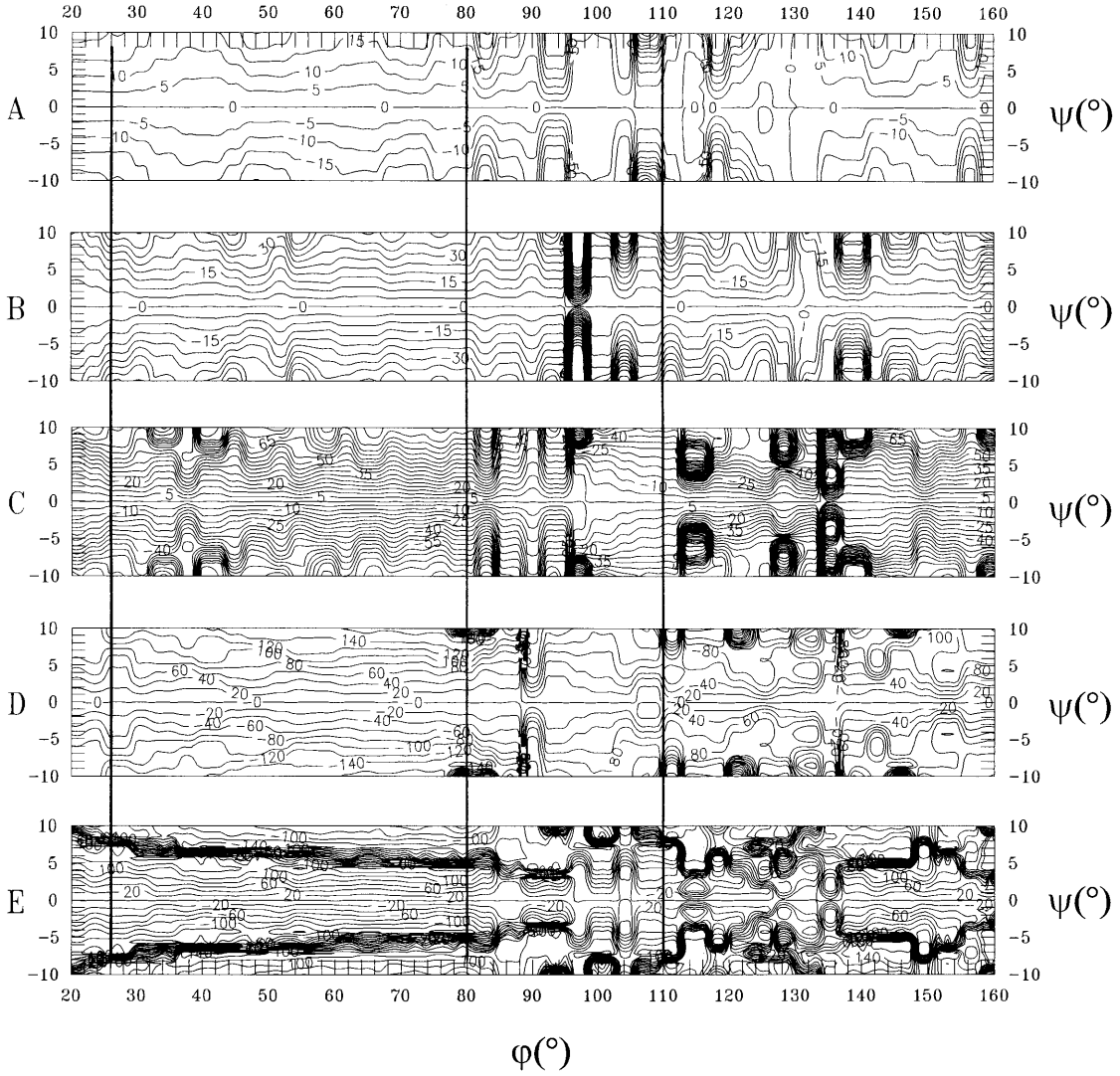

Fig. 2. Phase maps for water droplets with parallel polarization: A, d = 10 μm; B, d = 20 μm; C, d = 40 μm; D, d = 80 μm; E, d = 150 μm.

and the power of scattered light into the receiving aperture are three factors that define the reliability of the measurements; the optimization steps are therefore as follows: at first a proper off-axis angle is found for a linear phase–diameter relationship. This can be achieved by selecting a region of possibly straight contour lines in the phase maps. In fact, it can result in a linear phase–diameter relation if the texture of contour lines remains unchanged and the rate of change in line spacing is uniform relative to particle size changes. However, in an arrangement of off-axis detection this can be obtained only when straightness of contour lines exists. Next is an examination of the visibility and intensity to determine if they are high enough to ensure reliable signal processing.

Three cases are investigated: absorption-free water droplets, extremely absorbing metal particles, and droplets from an ink solution as weakly absorbent material, for which until now a suitable method for setting up ideal measurement parameters has been lacking. In the figures that follow, unless otherwise stated, the input data listed in Table 1 were used. In spite of the possibility of getting better results in the system optimization by locating the receivers unsymmetrically, I discuss only the case of symmetric arrangement of the detectors with respect to the y–z plane in the following subsections to highlight the effectiveness of the described method. In all the phase maps the horizontal and vertical directions correspond to the off-axis angle $\varphi(=\varphi_1=\varphi_2)$, which ranges from 20° to 160°, and the elevation angle $\psi(=\psi_1=-\psi_2)$, which ranges from −10° to 10°, respectively. The power of each incident laser beam is assumed to be 1 W. The waist diameter of the Gaussian beam at the measurement volume, which is dependent on the parameters of the sending optics, is valued at 324.2 μm. The intensity at the beam waist is the averaged value of the incident light power over the beam spot area.

A. Water Droplets

Water is a typical and most successfully investigated example for PDA applications. Routine off-axis angles in a commercially available instrument for characterizing water sprays are 30° and 60° with parallel polarization of incident waves (the electric vector of the incident beams is polarized parallel to the interference fringe plane in the measurement volume). From the point of view of geometrical optics, the refraction through water droplets gives the main contribution under such off-axis angles. An overview of the phase behavior of the scattered light in a more general sense can be obtained by applying the Lorenz–Mie theory. For this purpose, phase maps in the form of contours have been generated with Eq. (4) for five droplet diameters: $d = 10, 20, 40, 80$, and 150 μm. The results are shown in Fig. 2. The contour lines in Figs. 2A, 2B, and 2C have equal intervals so that the proportionality of the phase to the diameter can be viewed easily. Because there are too many lines for larger particles, the contours in Figs. 2D and 2E have as much as four times the interval as those in Figs. 2A, 2B, and 2C. It can be concluded that the suitable region of the off-axis angle lies between 26° and 80° because in this region the contour lines are relatively straight for all five sampled diameters. This means that there is a linearity of change of the phase value as a function of particle size.

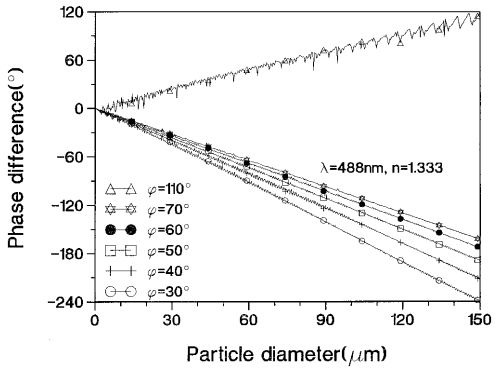

Fig. 3. Phase difference versus particle diameter for water droplets with parallel polarization.

Various off-axis angles have been selected and the results of phase differences versus diameter are shown in Fig. 3. In this figure the angle of 110° is chosen to indicate its unsuitability compared with other angles as a result of the disturbing oscillations in the corresponding curve, as can be expected from the phase maps in Fig. 2. One can also see that, at relative suitable positions, there are still many small fluctuations in the phase–diameter curves, which is consistent with the phase maps whose contour lines are not strictly straight. A further examination of the visibility (Fig. 4) and of the intensity (Fig. 5) shows that 30° and 60° are really two of the correct off-axis angles, that is, at these positions the visibility and the scattered power are high enough to ensure a high rate of signal acceptance.

B. Metal Particles

Metal particles have strong absorption and thus high reflectivity. These allow one to assume that the reflection is dominant in almost the entire off-axis angle range in the sense of geometrical optics. In this ex-

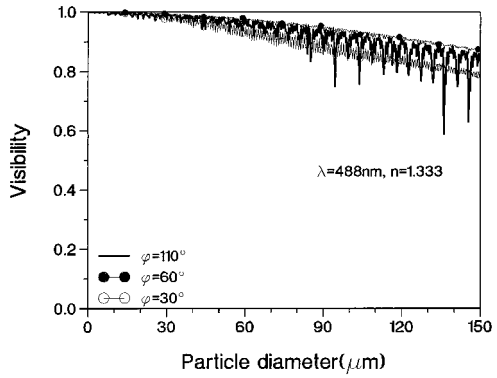

Fig. 4. Visibility versus particle diameter for water droplets with parallel polarization.

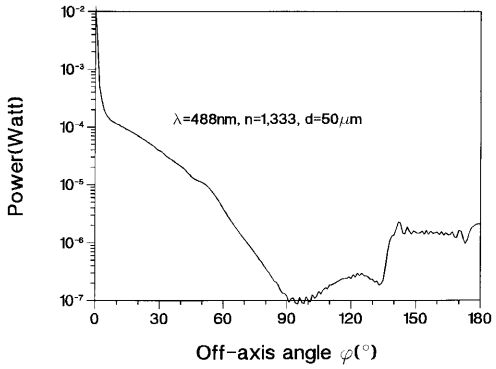

Fig. 5. Intensity versus off-axis angle for water droplets with parallel polarization.

ample the complex refractive index of the particles is assumed to be 1.5–i1.5, without losing general meaning. Because the parallel and perpendicular polarizations make a difference only in the small particle size range, four particle sizes (d = 10, 20, 40 and 80 μm) for parallel and two sizes (d = 10 and 20 μm) for perpendicular polarization were taken into account when the phase maps in Figs. 6 and 7, respectively, were generated. It is immediately clear that almost everywhere is suitable for positioning the detector aperture if the particles to be measured are larger than 10 μm. If smaller particles must be considered, the correct region is at $\varphi > 25°$ for perpendicular polarization and at $\varphi > 45°$ for parallel polarization. Similar to one's expectation from geometrical optics, the results from the Lorenz–Mie theory show that the perpendicular polarization is more suitable than the parallel one. The small particle range may be of more interest; hence the phase difference–diameter relations are figured in the range 0.01–30 μm as shown in Figs. 8 and 9. The suitability of perpendicular polarization and the expectation according to the phase maps are verified and clarified. At φ = 60°, particles with a diameter as small as 1.0 μm can be measured precisely. Also with regard to intensity, perpendicular polarization has advantages over parallel polarization (Fig. 10), whereas the visibility is the same for both (Fig. 11).

C. Droplets of the 25% Ink Solution

It is meaningful to be able to size optically absorbing particles, because in practice many fluids are neither free of absorption nor extremely absorbing. Droplets from black ink solutions of various concentrations, which can be considered to be homogeneous under the given experimental conditions, have been measured and examined.[6] The measuring system was calibrated by using the Lorenz–Mie theory, and it was demonstrated that the PDA equipment of routine arrangement is, with some limitations (the degree of lim-

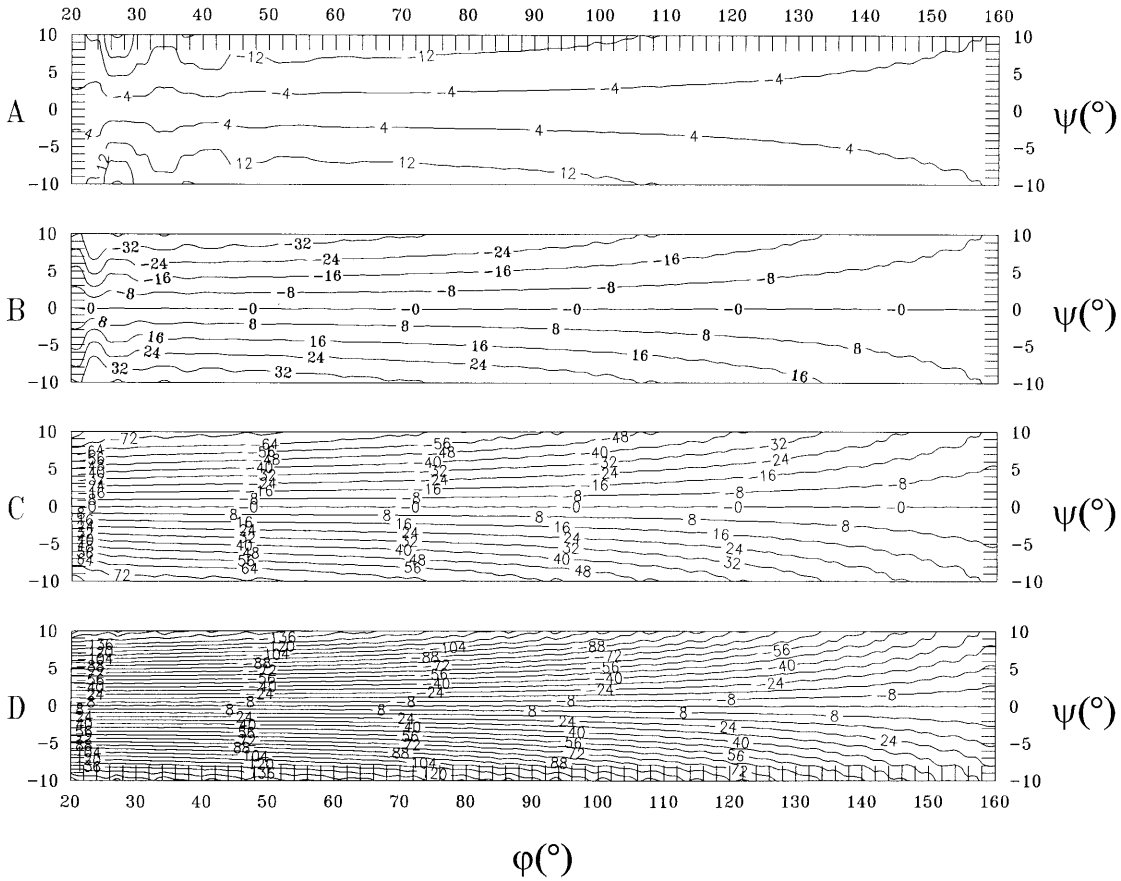

Fig. 6. Phase maps for metal particles with parallel polarization: A, d = 10 μm; B, d = 20 μm; C, d = 40 μm; D, d = 80 μm.

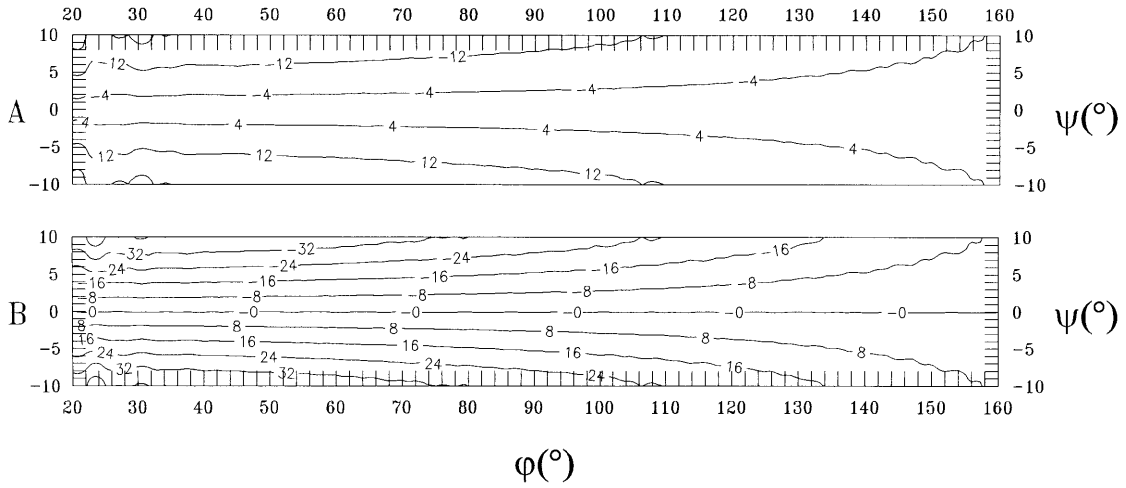

Fig. 7. Phase maps for metal particles with perpendicular polarization: A, $d = 10$ μm; B, $d = 20$ μm.

itation depends on the absorbing ability of the liquid), also applicable in sizing absorbant liquid droplets. The absorption of the 25% ink solution lies in the critical range and is the subject of this subsection—with a correct setup to remove the existing limitations. The measured complex refractive index of the ink solution is 1.3404–*i*0.0025.[6]

In this case it is difficult to imagine or to predict where one should allow for an aperture by using geometrical optics. Until now there has been no appropriate method to set up a PDA measuring system correctly and efficiently in such circumstances. Here it is demonstrated that the phase maps are adequate to serve as an efficient tool in finding the best apparatus configuration. In Figs. 12 and 13 the phase maps are generated for both polarizations. The sampled particle diameters are $d = 10, 20, 40, 80$ and 150 μm, corresponding to parts A, B, C, D, and E

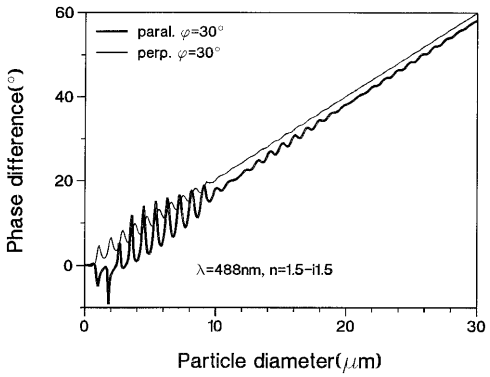

Fig. 8. Phase difference versus particle diameter for metal particles; φ = 30°.

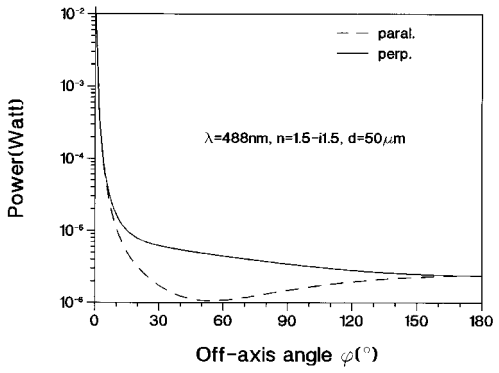

Fig. 10. Intensity versus off-axis angle for metal particles; $d = 50$ μm.

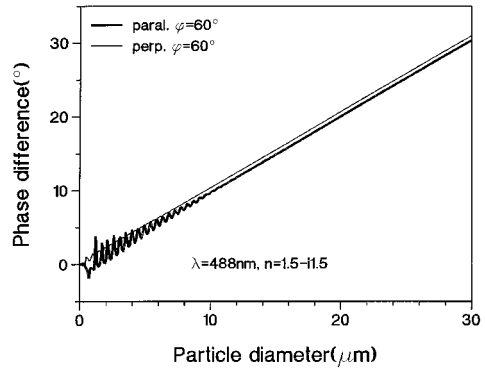

Fig. 9. Phase difference versus particle diameter for metal particles; φ = 60°.

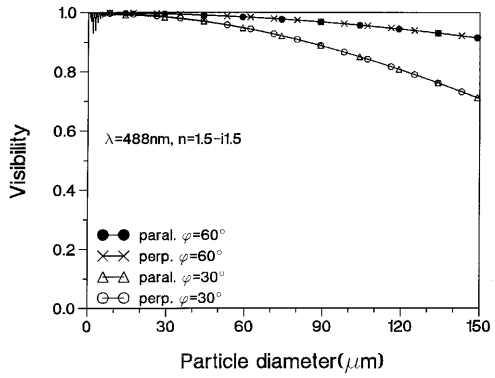

Fig. 11. Visibility versus particle diameter for metal particles.

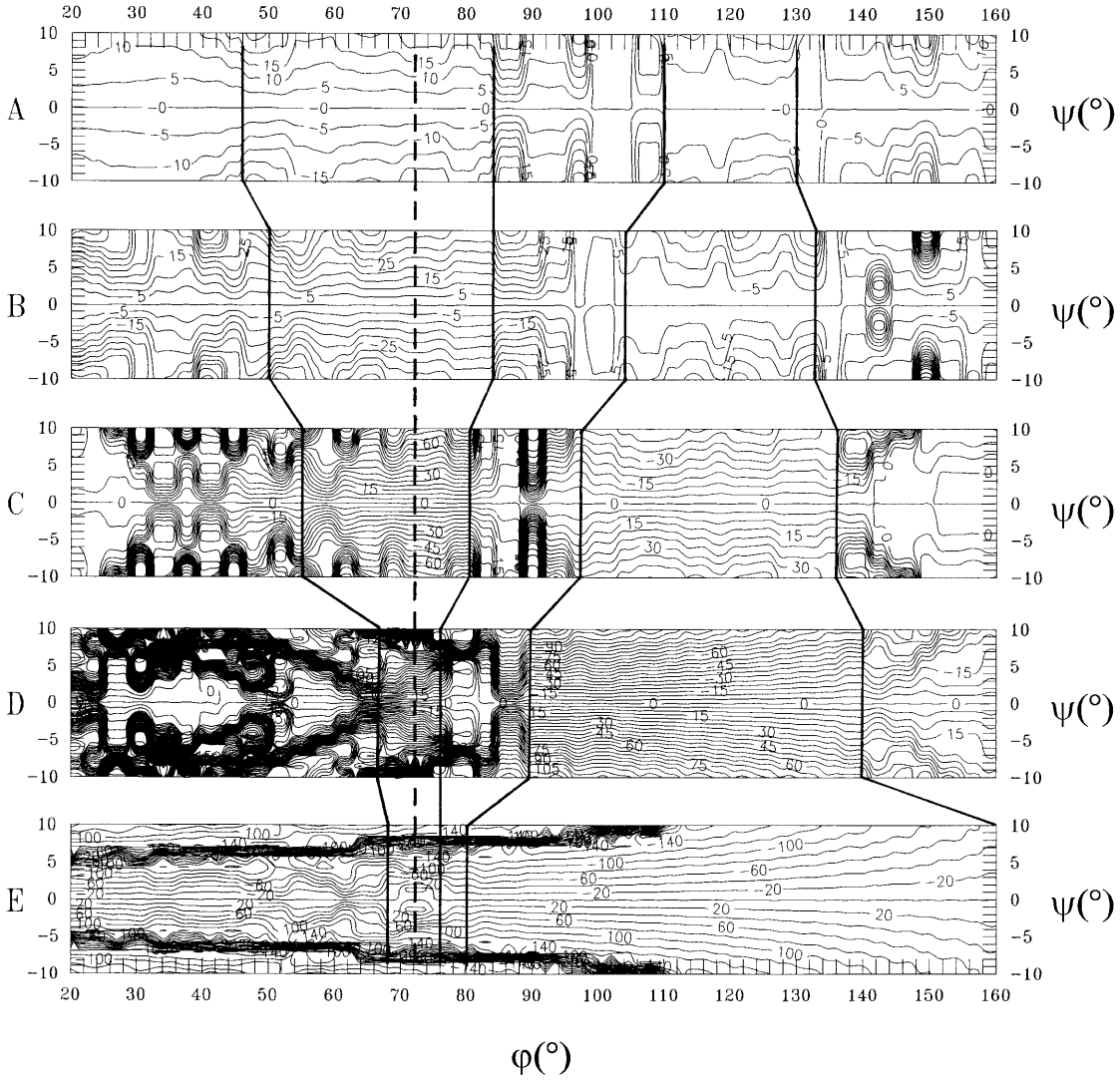

Fig. 12. Phase maps for ink solution droplets with parallel polarization: A, $d = 10$ μm; B, $d = 20$ μm; C, $d = 40$ μm; D, $d = 80$ μm; E, $d = 150$ μm.

in both figures. From A to D the contours have the same interval, making the proportional relation of phases to particle sizes clear. In E they are assigned with as much as four times the interval of that in the other four. It can be observed from Fig. 13 that under perpendicular polarization, the suitable region of the off-axis angle is reduced from nearly the whole region in E to 95–112° in A. Under parallel polarization (Fig. 12) there are two tendencies: in the backward direction ($\varphi > 90°$) the possible proper region of off-axis angle φ, corresponding to reflection, is reduced from the range of 80–160° in E to 110–130° in A, with bigger and more tortuous contours than in the case of perpendicular polarization. In the forward direction ($\varphi < 90°$) the possible region that corresponds to refraction reduces in reverse order from 46–84° in A to 66–76° in D. Careful observation reveals a change in the structure of contour lines in E at approximately 72°. This implies a change in the phase difference–diameter relation.

Based on this analysis, two off-axis angles of 72° and 100° were chosen to generate the phase difference–diameter curves. The calculated results are shown in Fig. 14. As analyzed above, the most suitable angle must be 100° under perpendicular polarization. Based on knowledge of phase maps, the 100° is not suitable for positioning detectors under parallel polarization, as is also indicated by the fluctuations in the corresponding curve in Fig. 14. It is worth mentioning the curve in Fig. 14 at $\varphi = 72°$ under parallel polarization. Under this angle the refraction is dominant to $d \simeq 90$ μm; above it the reflection is dominant. This phenomenon can be explained as follows: As the droplets are so small that the absorption is almost negligible, they can be regarded as refracting particles; with increasing particle size the effect of absorption becomes more and more noticeable until the droplets act as reflecting particles. This is what the change in the texture of contours in Fig. 12E means. It results in nonmonotonicity of the phase–diameter relationship if the range of particle sizes contains this transition posi-

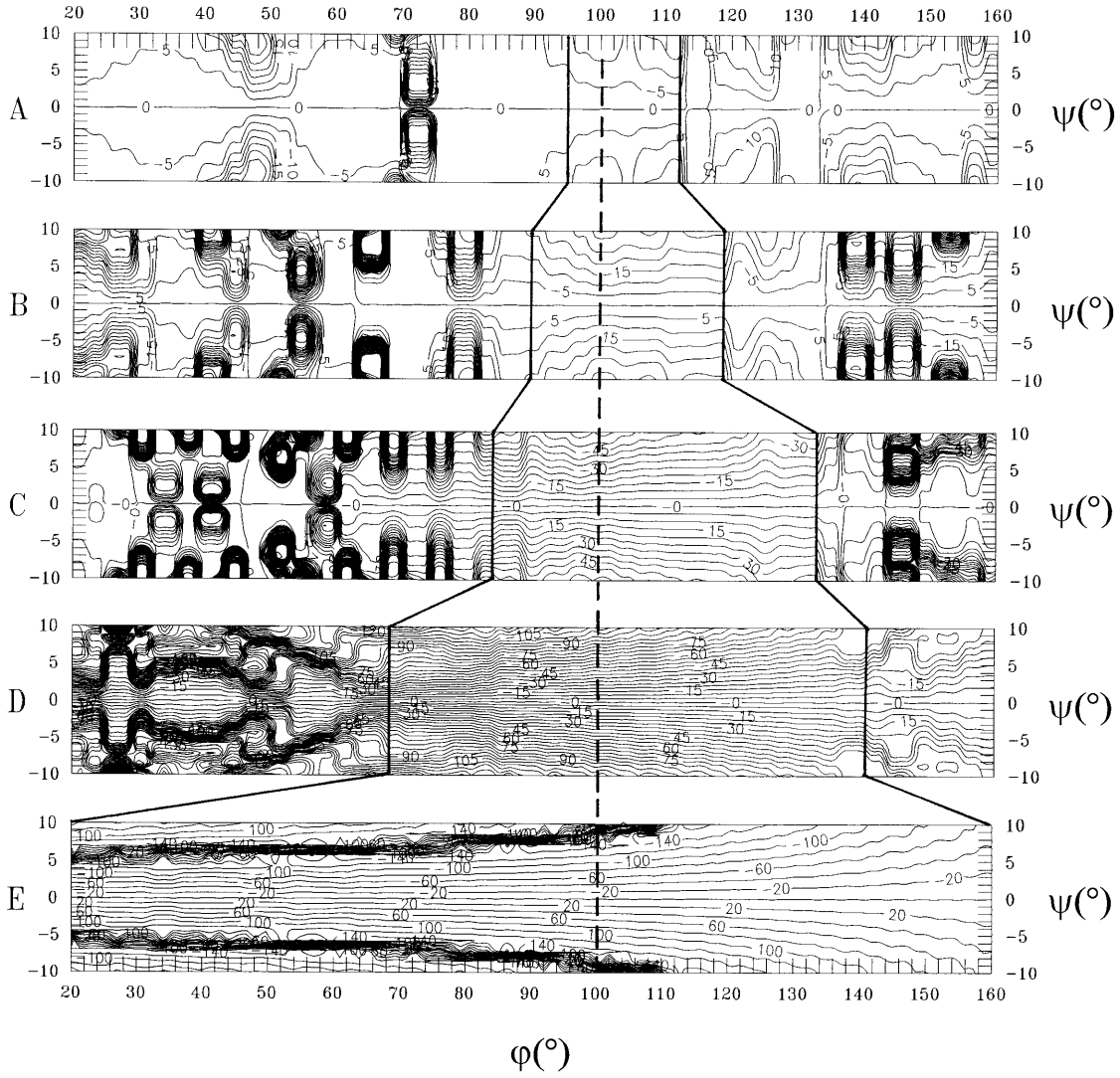

Fig. 13. Phase maps for ink solution droplets with perpendicular polarization: A, $d = 10$ μm; B, $d = 20$ μm; C, $d = 40$ μm; D, $d = 80$ μm; E, $d = 150$ μm.

tion. Also, the visibility (Fig. 15) indicates that 72° should not be selected. A final view at the distribution of scattered power in Fig. 16 confirms the 100° angle under perpendicular polarization as a suitable off-axis angle for measuring the 25% ink solution.

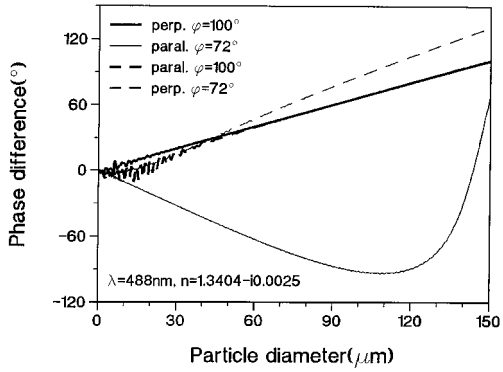

Fig. 14. Phase difference versus particle diameter for ink solution droplets.

4. Conclusions

Phase maps, together with information of visibility and intensity, provide one with an exclusive and clear picture of where signals can be detected. In especially difficult cases, such as for weakly and mildly absorbing particles, e.g., for droplets of the 25% ink solution, this is a helpful tool for determining an exact suitable position of a receiving aperture. The use of phase maps has the advantages that they deliver simple, direct, and unique knowledge about the phase distribution, which is the most important of the three factors that one can use to decide the performances of a PDA system. With this method one needs less computing time because no integration over the receiving aperture has to be carried out when generating the phase distributions and the phase maps have to be made for only a few particle sizes. For particle diameters of 10, 20, 40, 80 and 150 μm, computation for the five phase maps takes only a few minutes with a PC with a Pentium 90 type

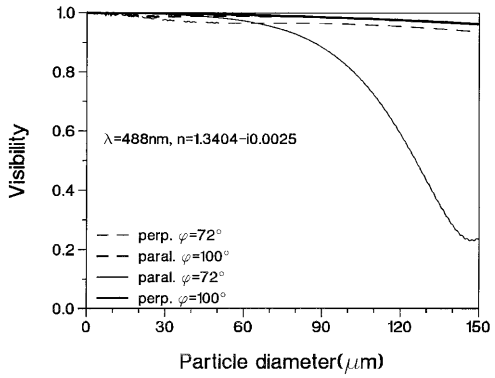

Fig. 15. Visibility versus particle diameter for ink solution droplets.

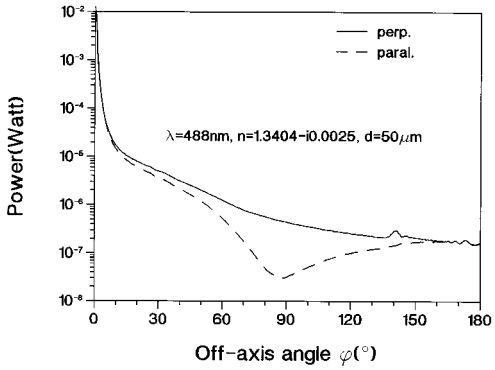

Fig. 16. Intensity versus off-axis angle for ink solution droplets; $d = 50$ μm.

of processor and with a Microsoft FORTRAN 4.0 compiler.

References

1. F. Durst and M. Zare, "Laser Doppler measurements in two-phase flows," in the *Accuracy of Flow Measurements by the Laser Doppler Method, Proceedings of the LDA Symposium, Copenhagen* (P.O. Box 70, DK-2740, Skovlunde, Denmark, 1975), pp. 403–429.
2. W. D. Bachalo and M. J. Houser, "Phase Doppler spray analyzer for simultaneous measurements of drop size and velocity distributions," Opt. Eng. **23,** 583–590 (1984).
3. M. Saffmann, P. Buchhave, and H. Tanger, "Simultaneous measurement of size, concentration and velocity of spherical particles by a laser Doppler method," presented at the Second International Symposium on Applications of Laser Anemometry to Fluid Mechanics, Lisbon, Portugal, 2–4 July 1984.
4. K. Bauckhage, "The phase-Doppler-difference-method, a new laser-Doppler technique for simultaneous size and velocity measurement. Part 1: description of the method," Part. Part. Syst. Charact. **5,** 16–22 (1988).
5. S. V. Sankar and W. D. Bachalo, "Response characteristics of the phase Doppler particle analyzer for sizing spherical particles larger than the light wavelength," Appl. Opt. **30,** 1487–1495 (1991).
6. U. Manasse, Z. Jiang, Th. Wriedt, and K. Bauckhage, "Application of the phase Doppler technique to optically absorbent liquids," in *Particle Size Analysis*, N. G. Stanley-Wood and R. W. Lines, eds. (The Royal Society of Chemistry, Cambridge, 1992), pp. 215–225.
7. G. Mie, "Beiträge zur Optik trüber Medien, speziell kolloidaler Metallösungen," Ann. Phy. (Leipzig) **25,** 377–445 (1908).
8. W. M. Farmer, "Measurement of particle size, number density, and velocity using a laser interferometer," Appl. Opt. **11,** 2603–2612 (1972).
9. W. P. Chu and D. M. Robinson, "Scattering from a moving spherical particle by two crossed coherent plane waves," Appl. Opt. **16,** 619–626 (1977).
10. N. S. Hong and A. R. Jones, "A light scattering technique for particle sizing based on laser fringe anemometry," J. Phys. D **9,** 1839–1848 (1976).
11. J. D. Pendleton, "Mie and refraction theory comparison for particle sizing with the laser velocimeter," Appl. Opt. **21,** 684–688 (1982).
12. A. A. Naqwi and F. Durst, "Light scattering applied to LDA and PDA measurements. Part 1: theory and numerical treatments," Part. Part. Syst. Charact. **8,** 245–258 (1991).
13. A. A. Naqwi and F. Durst, "Light scattering applied to LDA and PDA measurements. Part 2: computational results and their discussion," Part. Part. Syst. Charact. **9,** 66–80 (1992).
14. G. Gréhan, G. Gouesbet, A. Naqwi, and F. Durst, "Trajectory ambiguities in phase Doppler systems: study of a near forward and a near-backword geometry," Part. Part. Syst. Charact. **11,** 133–144 (1994).
15. H.-H. v. Benzon and P. Buchhave, "The phase-Doppler method applied to very small particles," Part. Part. Syst. Charact. **11,** 55–62 (1994).
16. Z. Jiang, "Simulation der Phasen-Doppler-Anemometrie anhand der Mie-Theorie: Beispielhafte Bestimmung geeigneter Systemparameter," Ph.D. dissertation (Universität Bremen, FB-4/VT, Bremen, Germany, 1994).
17. R. J. Adrian and W. L. Earley, "Evaluation of LDV performance using Mie scattering theory," in *Proceedings of the Symposium on Laser Anemometry* (University of Minnesota, Department of Conferences, Minneapolis, Minn., 1976), p. 426.
18. C. F. Bohren and D. R. Huffman, *Absorption and Scattering of Light by Small Particles* (Wiley, New York, 1983).
19. W. J. Wiscombe, "Mie scattering calculations; advances in technique and fast, vector-speed computer code," Rep. NCAR/TN-140+STR (National Center for Atmospheric Research, Boulder, Colo., 1979).